CRYSTAL GROWTH & DESIGN

UNIVERSITY OF BIRMINGHAM

Subscriber access provided by University of Birmingham

Article

Conformational Solvatomorphism in a [2]Catenane

Shobhana Krishnaswamy, Soumyakanta Prusty, Daniel Chartrand, Garry S Hanan, and Dillip K. Chand

Cryst. Growth Des., **Just Accepted Manuscript** • DOI: 10.1021/acs.cgd.0c00421 • Publication Date (Web): 20 Jul 2020

Conformational Solvatomorphism in a [2]Catenane

Shobhana Krishnaswamy,[†a] Soumyakanta Prusty, [†a] Daniel Chartrand,[b] Garry S. Hanan[b] and Dillip K. Chand*[a]

[a]Department of Chemistry, Indian Institute of Technology Madras, Chennai 600 036, India. Email: dillip@iitm.ac.in

[b]Department of Chemistry, University of Montreal, Montreal QC H3T-IJ4 (Canada)

[†] *These authors contributed equally to this work.*

ABSTRACT: The combination of a flexible pyridine-appended ligand (L1) with 4,4′-bipyridine (L2) and *cis*-protected Pd(II) units, $Pd(L')(NO_3)_2$ in water yielded a concentration-dependent equilibrium mixture of the corresponding [2]catenanes $[Pd_2(L')_2(L1)(L2)]_2(NO_3)_8$ and their constituent macrocycles $[Pd_2(L')_2(L1)(L2)](NO_3)_4$. The *cis*-protecting units (L′) used were ethylenediamine (en), tetramethylethylenediamine (tmeda), 2,2′-bipyridine (bpy) and 1,10-phenanthroline (phen). Crystallization of the [2]catenanes via slow evaporation of their $CH_3CN:H_2O$ (1:1) solutions yielded a single crystalline form in the case of $[Pd_2(2,2'\text{-}bpy)_2(L1)(L2)]_2(NO_3)_8$ and two concomitant crystalline forms (solvates) in the case of $[Pd_2(phen)_2(L1)(L2)]_2(NO_3)_8$. The formation of the [2]catenane is facilitated by noncovalent interactions such as N-H…O, C-H…O, C-H…π contacts and π…π stacking. The solvates of $[Pd_2(phen)_2(L1)(L2)]_2(NO_3)_8$ revealed differences in the orientation of the amide carbonyl group and conformational differences in the ligands and phen units in the macrocycles and may thus be termed conformational solvatomorphs. The molecular packing in all the structures was found to be driven by intermolecular π…π stacking interactions between the aromatic rings in their *cis*-protected Pd(II) units. However, due to the awkward shape of the molecules the closest 2,2′-bpy and phen units in all the structures overlap differently rather than the commonly observed "head-to-tail" or head-to-head" modes.

INTRODUCTION

Polymorphism is the ability of a compound to exist in two or more crystalline forms, which exhibit differences in solid-state properties such as melting point, solubility, density and solid-state reactivity.[1-3] The occurrence of different conformers of the same molecule in the different crystal forms is referred to as conformational polymorphism.[4,5] Solvatomorphism is a related phenomenon where a solvent cocrystallizes with the compound in its crystal lattice. Solvatomorphs may show differences in molecular packing as compared to the solvent free forms and among each other. Instances of polymorphism and solvatomorphism in active pharmaceutical ingredients (APIs) have been extensively studied because of the possible effects on their stability and bioavailability.[6,7] Although the incidence of polymorphism and solvatomorphism in small organic molecules is well documented, these phenomena have also been observed in larger molecular systems, including proteins. A statistical study of polymorphism using the Cambridge Structural Database (CSD)[8] revealed no connection between the structural features of molecules such as size, hydrogen bonding ability, conformational flexibility and their propensity to yield multiple crystalline forms.[9]

Martins and coworkers recently described conformational polymorphs of a rotaxane and investigated the differences between them at the intramolecular level.[10] Baumes *et al*. obtained two conformationally different crystal structures of a rotaxane in separate experiments,[11] while Mezei *et al*. studied the crystal structures of polymorphs and solvatomorphs of pseudorotaxanes.[12] Stoddart and coworkers isolated four crystalline forms of a [3]catenane composed of two cyclobis(paraquat-*p*-phenylene) rings threaded into a dinaphtho[50]crown-14 macrocycle.[13] The formation of these solvatomorphs was attributed to the innate flexibility of the framework of the [3]catenane. These large systems belong to the class of mechanically interlocked molecules (MIMs) and are challenging synthetic targets, exhibit intriguing structural features, dynamic

behavior and find application as molecular machines and sensors.[14-19] [2]Catenanes are a class of MIMs composed of two rings interlocked via noncovalent interactions such as hydrogen bonding,[20,21] halogen bonding,[22-24] aromatic donor acceptor interactions[25-27] or synthesized using templates.[28-33] Transition metal ions can also be used in combination with chosen ligands to prepare metallocycles in high yield, which can undergo catenation, promoted by various types of donor-acceptor interactions.

We recently described the crystal structures of solvatomorphs of tetranuclear Pd(II) based molecular squares (Figure 1a) of the general formula $[Pd(L')(4,4'\text{-bpy})]_4(OTs)_8$ [where L′ represents 2,2′-bipyridine (bpy) or 1,10-phenanthroline (phen)] with emphasis on the modes of molecular packing adopted by the different crystalline forms.[34] The molecular packing in these structures was driven by intermolecular π…π stacking interactions between aromatic rings of the 2,2′-bpy and phenanthroline units. The present work describes the reaction of a flexible, pyridine-appended ligand, rigid 4,4′-bipyridine and *cis*-protected Pd(II) units (in 1:1:2 ratio) in water. A concentration-dependent equilibrating mixture of heteroleptic metallomacrocycles and the corresponding [2]catenanes (Figure 1b,c) was obtained. Crystals of the [2]catenanes containing 2,2′-bpy and 1,10-phenanthroline units were obtained upon slow evaporation of their acetonitrile-water solutions. A pair of solvatomorphs was obtained for the [2]catenane where 1,10-phenanthroline moieties were present in the *cis*-protected Pd(II) units, which showed differences in the orientation of the amide carbonyl groups and aromatic rings of the ligand and *cis*-protecting agent. These crystal structures provided us with an opportunity to examine the molecular packing in a tetranuclear complex, where the Pd(II) square planes are not coplanar unlike those in the Pd(II) molecular squares. The pairs of Pd(II) square planes present in the two interlocking macrocycles of the [2]catenane lie in two different planes, oriented nearly orthogonal to each other.

In the [2]catenanes, π…π stacking interactions were observed between the closest 2,2′-bpy and phenanthroline units, which do not overlap in the commonly observed "head-to-head" or "head-to-tail" manner.[35] We briefly describe the synthesis of the [2]catenanes, their characterization in the solution and solid states, analyses of their crystal structures and the differences in the crystal structures and molecular packing of the conformational solvatomorphs in the following sections.

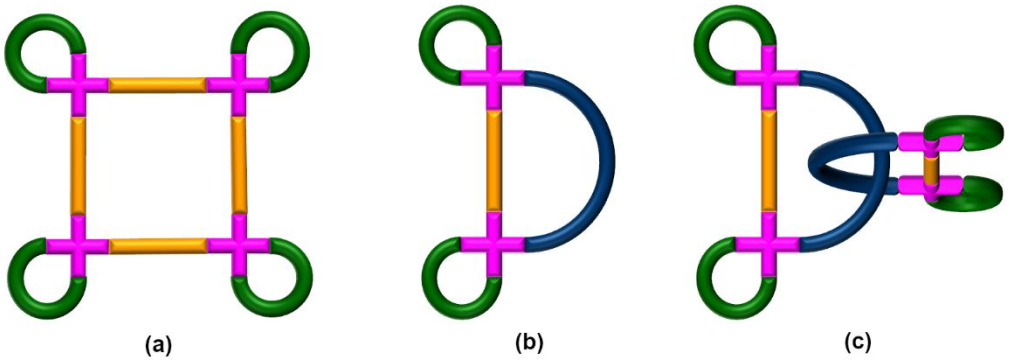

Figure 1. Schematic representations of *cis*-protected Pd(II) directed self-assembled complexes: (a) molecular square, (b) heteroleptic metallomacrocycle and (c) the corresponding [2]catenane. (Key: green – *cis*-protecting agent; pink – Pd(II) and its square plane; orange – 4,4′-bpy; blue – flexible pyridine-appended ligand.)

RESULTS AND DISCUSSION

Ligand **L1** upon crystallization from acetone and acetonitrile-methanol solutions produced two different solvated crystals belonging to the space groups *R*-3 and $P2_1/n$, respectively.[36] The molecules in both solvates adopt approximately *anti*-conformation in the solid state, with respect to the two isonicotinamide moieties, where the pyridine rings are oriented in opposite directions (Figure 2). The torsion angle C(*Ar*)-C(H_2)-N(*H*)-C(=*O*) in the acetone solvate (88°) is smaller in magnitude than that observed in the hydrate (110°).

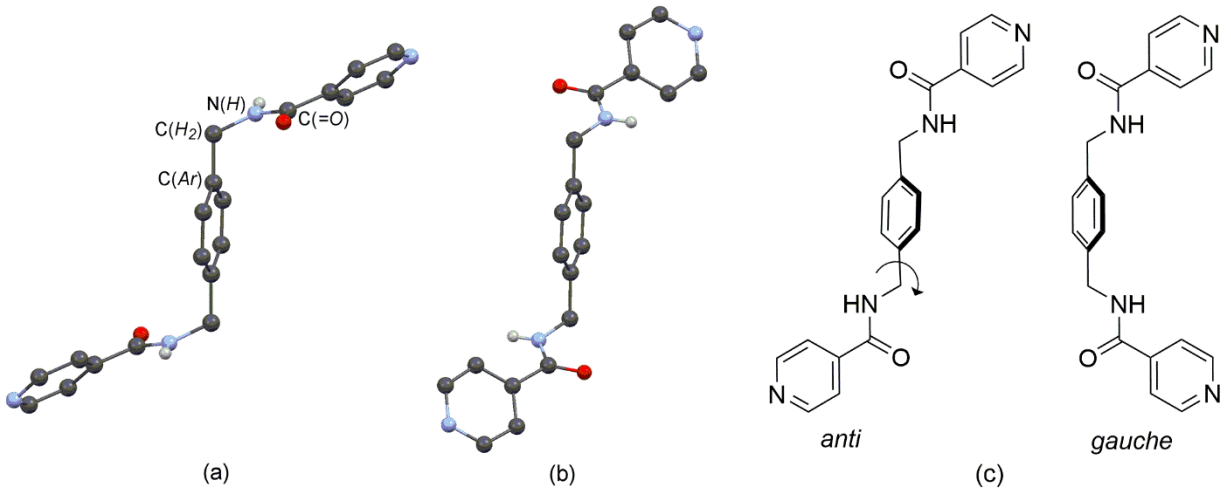

Figure 2. Conformation of the molecules (from single crystal structures) of the ligand **L1** in its (a) acetone solvate (SUNWEE)[8] and (b) hydrate (SUNWII).[8] (c) Chemical drawings of the *anti* and *gauche* conformations of the ligand. Hydrogen atoms other than the amide N-H atoms are omitted for clarity.

Synthesis and characterization of the macrocycle and [2]catenane. The reaction of **L1**, 4,4′-bipyridine (**L2**) and *cis*-protected Pd(II) units resulted in the formation of the heteroleptic macrocycles **1a-d**, when DMSO was the medium of complexation (Scheme 1). A concentration-dependent equilibrating mixture of the macrocycles (**1a-d**) and the corresponding [2]catenanes (**2a-d**) was obtained when the reaction was performed in water. The formation of the macrocycle and the [2]catenane requires the ligand to adopt the *gauche* conformation which is readily achieved by rotation about the C(*Ar*)-C(H_2) bond. In general, amides are structurally less flexible than the corresponding esters due to restricted rotation about the amide bond. The amide hydrogen and carbonyl oxygen atoms may engage in hydrogen bonding interactions with guest or solvent molecules.

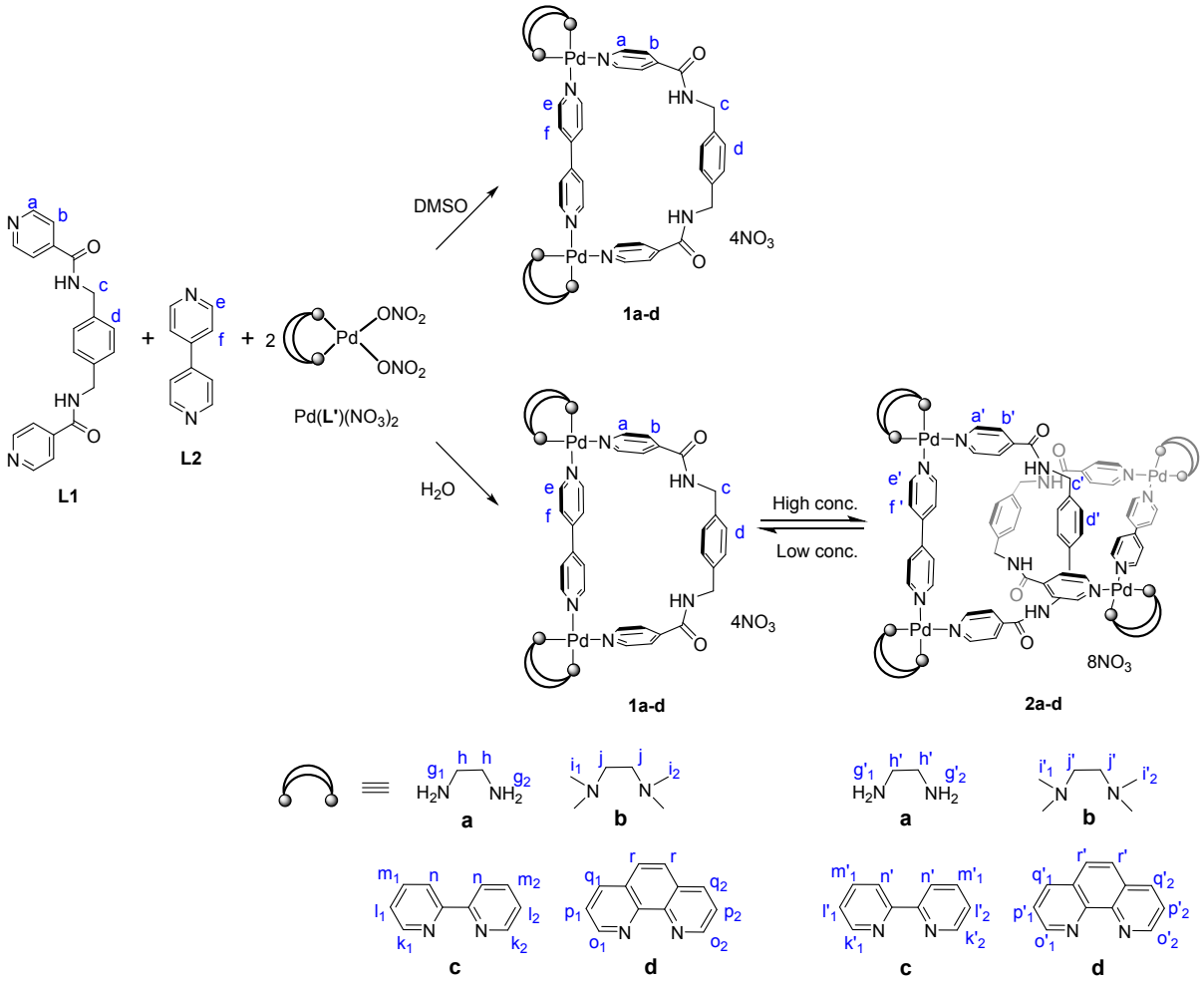

Scheme 1 Synthesis of the metallomacrocycles/[2]catenanes, **1a-d**/**2a-d**.

^{1}H NMR spectra (Figure 3) recorded for the complexes **1a-d** in DMSO-d_6 revealed a downfield shift in the signals of the H_a and H_b protons of the ligand **L1** and H_e and H_f protons of **L2** upon complexation. No significant change was observed in the chemical shifts of the protons corresponding to the phenyl and methylene groups of the ligand. The protons of the *cis*-protecting agent become non-equivalent after the formation of the heteroleptic macrocycles due to the loss of their plane of symmetry. The complexes were characterized by 1D and 2D NMR spectroscopy. (Figures S2-S23).

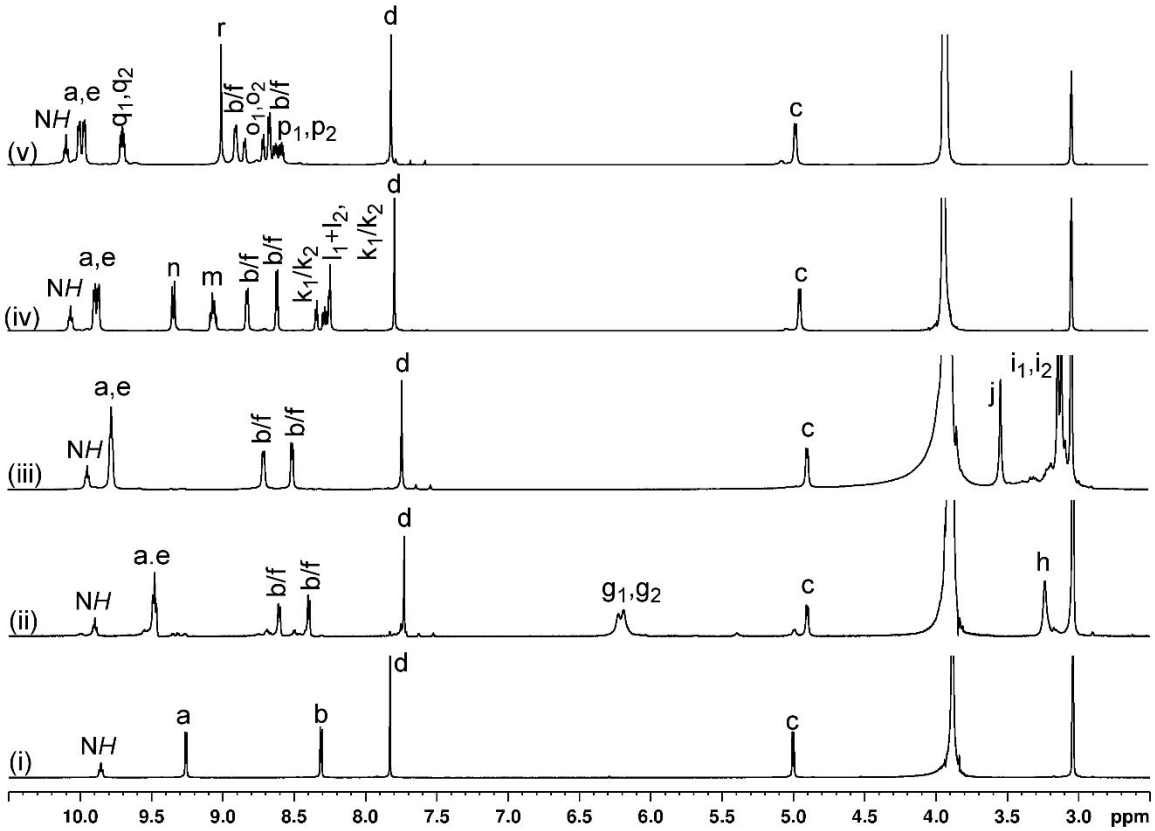

Figure 3. ^{1}H NMR spectra ([D6]DMSO, 25 °C, TMS as an external standard) of: (i) **L1**; and metallomacrocycles (ii) **1a**; (iii) **1b**; (iv) **1c** and (v) **1d**. [Concentration with respect to Pd(II) source: 10 mM for **1a-d**].

^{1}H NMR spectra for the complexes prepared at various concentrations in D_2O each showed two sets of peaks which belong to the macrocycle and [2]catenane, respectively (Figure 4). The signals of the methylene protons ($H_{c'}$) and phenyl hydrogens ($H_{d'}$) of one set appear upfield as compared to those of the second set (H_c and H_d). This is due to [2]catenane formation and occurs because of the influence of the diatropic ring currents of five aromatic rings of one interlocked macrocycle upon the other and *vice versa* as established earlier for a comparable catenane **3** (Scheme 2).[37] The composition and solution behavior of catenane **3** is comparable with that of the catenane **2c** and the notable structural difference is in terms of ester functionalities in the former and amide in the latter. The chemical shifts of the macrocycles **1a-d** and [2]catenanes **2a-d** and their differences are

summarized in Table S1. The complexes were characterized by 1D and 2D NMR spectroscopy (Figures S24-S51). Evidence for the presence of the two species was also obtained from 2D DOSY NMR spectra recorded for the four sets of equilibrium mixtures of macrocycle and [2]catenane (Figures S52-S55).

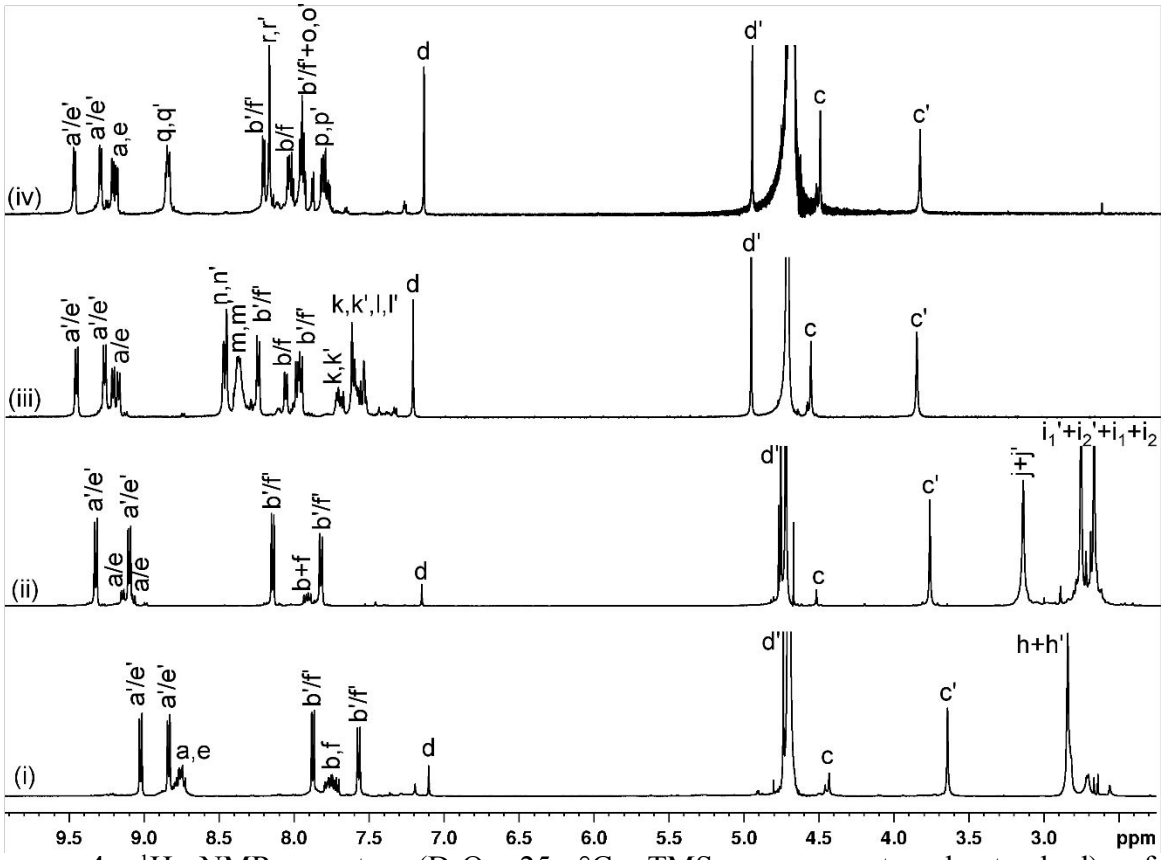

Figure 4. ^{1}H NMR spectra (D_2O, 25 °C, TMS as an external standard) of the metallomacrocycle/[2]catenae mixtures: (i) **1a**/**2a** (40 mM); (ii) **1b**/**2b** (50 mM); (iii) **1c**/**2c** (10 mM) and (iv) **1d**/**2d** (12 mM). Values in parentheses denote concentrations of the solutions with respect to Pd(II) source.

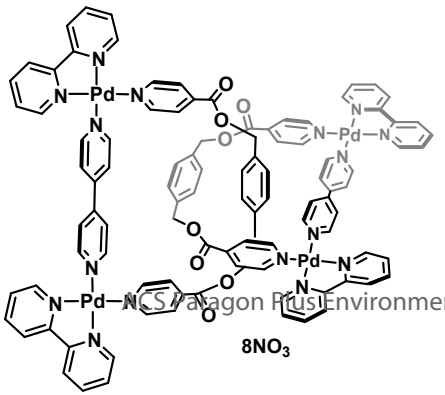

Scheme 2 Chemical structure of the [2]catenane **3**.

The macrocycle diffused faster than the [2]catenane due to its smaller size and hence, the DOSY study assisted assignment of the two sets of signals observed in the ^{1}H NMR spectra. The concentration-dependent equilibrium between the macrocycle and [2]catenane in water was studied by recording the ^{1}H NMR spectra of the complexes in D_2O at various concentrations (Figures S56-S59). The plot of percentage of the rings present as [2]catenane/macrocycle as a function of the concentration for all the equilibrium mixtures (Figure S60) shows that at high concentration, the [2]catenane is present in larger amounts while the macrocycles are the dominant species in dilute solutions. The equilibrium constants for the mixtures were calculated using ^{1}H NMR spectra recorded at different concentrations (Table S2). The measured diffusion coefficients of the macrocycles and corresponding [2]catenanes and the estimated equilibrium constants for their mixtures are summarized in Table 1. Additional evidence for the formation of the macrocycle and [2]catenane was obtained from cold spray ionization mass spectrometry data (CSI-MS) (Figures S61-S77). The isotopic patterns for the fragments showed good correspondence with the theoretically predicted distributions.

Table 1. Summary of equilibrium constants and diffusion coefficients estimated for the equilibrium mixtures of complexes.

Complexes	K_c ($mmol^{-1}L$)	D (m^2s^{-1})	
		Macrocycle	[2]Catenane
1a/2a	0.89 ± 0.05	(2.82 ± 0.03) × 10^{-10}	(2.22 ± 0.01) × 10^{-10}
1b/2b	1.58 ± 0.08	(2.69 ± 0.04) × 10^{-10}	(2.07 ± 0.01) × 10^{-10}
1c/2c	0.18 ± 0.04	(2.724 ± 0.002) × 10^{-10}	(2.05 ± 0.02) × 10^{-10}
1d/2d	0.12 ± 0.03	(2.47 ± 0.03) × 10^{-10}	(2.01 ± 0.01) × 10^{-10}

Crystal structures of the [2]catenanes Attempts to crystallize the macrocycles **1a-d** and the [2]catenanes **2a** and **2b** via slow evaporation of their aqueous solutions or vapor diffusion experiments were not fruitful. Crystals of the [2]catenanes **2c** and **2d**, however, were spontaneously obtained by slow evaporation of CH_3CN-H_2O (1:1 *v*/*v*) solutions containing the mixture of complexes **1c/2c** and **1d/2d**, respectively. This could be attributed to the fact that concentrated aqueous media favor the formation of these catenanes.[38] Crystals of solvatomorphs **2dI** ($C2/c$) and **2dII** ($P2_1/n$) were obtained concomitantly from a CH_3CN-H_2O solution of the complex **2d**. We recently reported[37] the crystal structure (CSD[8] refcode: RUSZAI) of the tetranuclear [2]catenane (**3**) for which a chemical drawing is shown in scheme 2. An elaborate discussion on the crystal structure of **3**, not included in the earlier report, is warranted here. Comparisons are drawn between the crystal structures and molecular packing in **2cI**, **2dI, 2dII** and **3**. All the [2]catenanes crystallized in monoclinic space groups. The central phenyl ring of the ligand of one macrocycle lies inside the cavity of the second macrocycle and the 4,4′-bpy units are present outside in all the crystal structures. The asymmetric unit in **2cI** (Figure S78) and **2dI** (Figure S79) contained a single macrocycle, whereas a pair of interlocked symmetry independent macrocycles were present in the asymmetric unit in crystals of **2dII** (Figure S80) and **3**.[37] The

crystals of **2cI** and **2dI** were highly unstable and rapidly lost crystallinity when exposed to air. The positions of disordered anions and solvent molecules in these crystals could not be determined from the difference Fourier map, hence electron density corresponding to these moieties was squeezed.[39] The crystallographic data are briefly summarized in Table2 (see Table S3 for details). The details of structure solution and ORTEPs are available in the Supporting Information.

Table 2. Summary of crystallographic data for crystals of **2c** and **2d**.

	2cI	**2dI**	**2dII**
Chemical Formula	$C_{50}H_{42}N_{10}O_2Pd_2$	$C_{54}H_{42}N_{10}O_2Pd_2$	$C_{108}H_{146}N_{28}O_{59}Pd_4$
M_r	1027.73	1075.77	3206.12
Temperature (K)	296(2)	296(2)	100
Crystal system	Monoclinic	Monoclinic	Monoclinic
Space group	*C*2/*c*	*C*2/*c*	$P2_1/n$
a (Å)	13.1208(5)	13.419(5)	12.6708(11)
b (Å)	28.8866(10)	28.900(5)	29.645(2)
c (Å)	37.6371(11)	37.540(5)	36.539(3)
α (°)	90	90	90
β (°)	94.437(2)	96.995(5)	99.532(2)
γ (°)	90	90	90
V (Å^3)	14222.3(8)	14450(6)	13535.5(19)
Z D_{calc} (g cm^{-3})	8 0.960	8 0.989	4 1.573
Unique reflns	10247	5746	30912
R_{int}	0.0413	0.0368	0.050
GoF	1.052	1.108	1.026
$R_1[I > 2\sigma(I)]$	0.0970	0.0960	0.0683
$WR_2[I > 2\sigma(I)]$	0.2972	0.2653	0.1858
R_1_all data	0.1575	0.1435	0.0851
Wr_2_ all data	0.3509	0.3480	0.2048
CCDC No.	1988795	1988797	1988796

Conformations of the macrocycles in the [2]catenanes. Scrutiny of the conformational differences in the macrocycles that form the [2]catenane reveals the dissimilarities in the crystal structures.

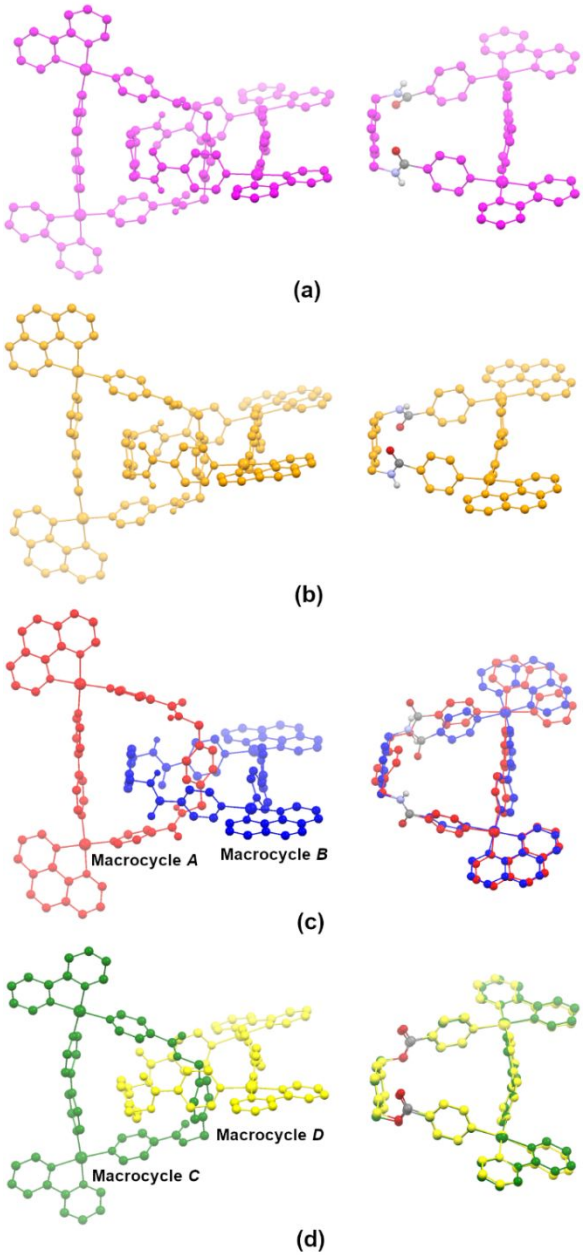

Figure 5. Crystal structures of the [2]catenanes and overlaps of the catenating macrocycles in (a) **2cI**; (b) **2dI**; (c) **2dII** and (d) **3** show the orientation of the ester and amide carbonyl groups in the macrocycles.

In each ring, the two ester/amide carbonyl groups may be aligned in *syn* (C=O groups facing approximately the same direction) or *anti* (C=O facing approximately the opposite directions) mode as substantiated with the measured torsion angles O=C- - - -C=O (Table 3) for ligand **L1** in its crystals and in the macrocycles in **2cI**, **2dI**, **2dII** and **3**. Since a single macrocycle is present in the asymmetric unit of the crystal structures of **2cI** and **2dI**, respectively, the [2]catenanes are composed of identical rings. The amide carbonyl groups are oriented *anti* to each other in **2cI** (Figure 5a) and **2dI** (Figure 5b), whereas the ester carbonyl groups of the catenating rings in **3** are oriented *syn* to each other (Figure 5d, Table 3). However, the overlay of the catenating rings in the crystals of **2dII** reveals that in macrocycle *A* (red, Figure 5c), the amide carbonyl groups are aligned *anti*, while in macrocycle *B* (blue, Figure 5c), they are aligned *syn* to each other. These differences in the orientation of the carbonyl groups in the crystal structures of **2cI**, **2dI**, **2dII** and **3** revealed that their crystals contain equal proportions of enantiomorphic [2]catenanes.

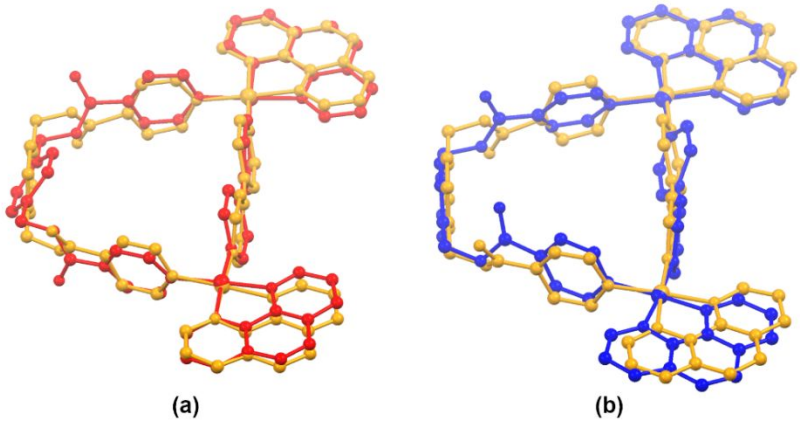

Figure 6. Overlaps of the macrocycle (yellow) in the crystals of **2dI** with the symmetry independent (a) macrocycle *A* and (b) macrocycle *B* in crystals of **2dII** show the conformational differences in the solvatomorphs.

Further, the overlaps of the macrocycle in crystals of **2dI** and macrocycles *A* (Figure 6a) and *B* (Figure 6b) in **2dII** revealed differences in the orientation of the central phenyl ring of the ligand and the rings of the phenanthroline units of the two macrocycles in **2dII**. Therefore, **2dI** and **2dII** are conformational solvatomorphs. A single sharp set of peaks is observed in the ^{1}H NMR spectrum for **2dII**, suggesting that an averaged picture of the different conformations is seen in the solution state. The orientations of these carbonyl groups influence the hydrogen bonding interactions between the interlocked molecules.

The torsion angles C(*Ar*)-C(H_2)-N(*H*)-C(=*O*) measured for the ligand **L1** in its crystals and in the macrocycles in **2cI**, **2dI**, **2dII** and **3** are also summarized in Table 3. Two different values of the angle were measured for the ligand in the crystals of the [2]catenanes, indicating the unsymmetrical orientation of the two pyridyl arms of the coordinated ligand. These differences may be due to the noncovalent interactions between the catenating rings during the process of forming the interlocked structure and the interactions of the [2]catenane with anions and solvent molecules.

Table 3. Comparison of the geometry of the ligand in the [2]catenanes.

Crystal	∠**O**=**C**- - - -**C**=**O** (°)	∠**C**(*Ar*)-**C**(H_2)-**N**(*H*)/**O**-**C**(=*O*) (°)
Ligand **L1** (acetone solvate)	-180	88.0(2), -88.0(2)
Ligand **L1** (hydrate)	180	110.8(1), -110.8(1)
2cI	-118(1)	92(1), 106(2)
2dI	-120(3)	90(3), 110(3)
2dII (Macrocycle *A*)	125.7(6)	-86.4(7), -110.5(7)
2dII (Macrocycle *B*)	-14.5(5)	-76.7(7), -88.4(6)
3 (Macrocycle *C*)	-2(2)	-90(2), 94(2)
3 (Macrocycle *D*)	-3(2)	93(1), -95(2)

Interactions between the interlocked rings The catenating rings in **2cI** (Figure 7a) and **2dI** (Figure 7b) interact via C-H···π interactions (C20-H20···Cg5 in **2cI** and C21-H21···Cg7 in **2dI**) between the hydrogen atoms of the central phenyl ring and the pyridine rings of the ligand and weak π···π interactions between the aromatic rings of the ligands. The interplanar distances between the aromatic systems, (4,4′-bpy)-(phenylene)-(phenylene)-(4,4′-bpy), and the dihedral angles between these planes span the range 4.27–4.69 Å and 8-14° (Table S4).

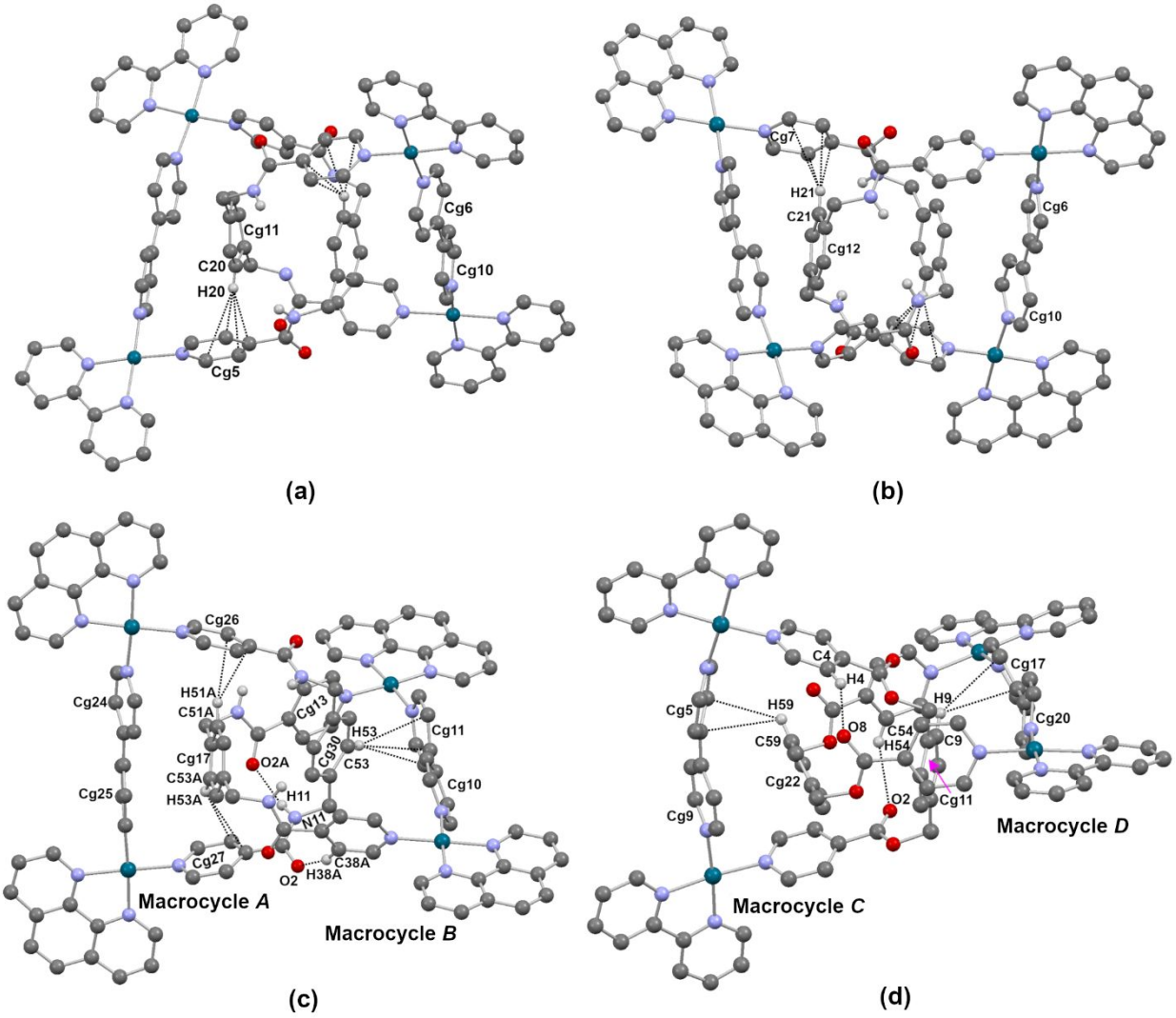

Figure 7. Intermolecular interactions between pairs of interlocked molecules in crystals of (a) **2cI**; (b) **2dI**; (c) **2dII** and (d) **3**. Solvent molecules, anions and hydrogen atoms not involved in hydrogen bonding are omitted for clarity.

The interlocked rings (macrocycles *A* and *B*) in **2dII** interact via a short and linear N-H···O (N11-H11···O2A) interaction between the amide hydrogen atom of ring *A* and carbonyl oxygen atom of ring *B*. The interlinking of the rings is supported by C-H···O (C38A-H38A···O2), C-H···π (C51-H51A···Cg26, C53A-H53A···Cg27, C53-H53···Cg11) and weak π···π interactions (Figure 7c). The interplanar distances between the aromatic systems and the dihedral angles between the planes of these aromatic rings lie in the range of 4.32-4.63 Å and 9-46°, respectively (Table S4).

The interlocked rings (macrocycles *C* and *D*) in **3**[37] interact through a pair of C-H···O interactions (C4-H4···O8 and C54-H54···O2) between the pyridyl hydrogen atoms and the carbonyl oxygen atoms of the ester groups. The interlocking is supported by weak π···π interactions between the aromatic systems (Figure 7d). The interplanar distances between the aromatic systems and the dihedral angles between the planes of these aromatic rings lie in the range 4.65–4.82 Å and 19-45°, respectively (Table S4). The amide hydrogen atoms in **2cI** and **2dI** are not involved in significant short contacts with the cationic portion of the molecule, unlike those in **2dII**. The interlocked macrocycles in **2dII** are held together by stronger hydrogen bonding interactions than those observed between the catenating rings in **3**. The interplanar distances between the stacked aromatic systems at the core of the catenane are marginally shorter in the structures of **2c** and **2d** as compared to those observed in **3**.

Packing of the [2]catenanes in their crystals. Despite the differences in the conformation of the interlocked molecules, the apparent similarities in the patterns of molecular self-assembly in the solid state are a consequence of the noncovalent interactions between the *cis*-protecting agents at the metal centers of adjacent molecules. The structures of the [2]catenanes reveal that the *p*-phenylene groups lie buried in the core of the molecule and the 2,2′-bpy/phen units lie at the corners of an imaginary irregular tetrahedron with vertices corresponding to the Pd(II) metal

centers. Views of the packing of the [2]catenanes in the crystals of **2cI** (Figure 8a) and **3** (Figure 9a) along the *a* and *b* axes respectively, reveal association of the molecules through weak π…π stacking interactions (~4.6 – 4.7 Å)[40] between the closest 2,2′-bpy units, forming chains along the *c*-axis. The chains in **2cI** are linked by weak stacking interactions (~4.7 Å) between the pyridine rings of the ligands along the *a*-axis (Figure 8b) and weak π…π stacking between 2,2′-bpy units along the *b*-axis in **3** (Figure 9b).

Zaric and coworkers studied the stacking interactions between square planar metal complexes containing 2,2′-bpy ligands by analyzing crystal structures in the CSD[8] and performing DFT calculations.[35] They defined the orientations of the interacting metal complexes as "head-to-head" or "head-to-tail" using a measured torsion angle, T_1.[35] T_1 is defined as the Ω_{C1}–M_1–M_2–Ω_{C2} angle where Ω_{C1} and Ω_{C2} represent the centers of the chelate rings in the two 2,2′-bpy units, respectively, and M_1 and M_2 are the corresponding metal ions.[35] The structures where T_1 lies between 0°-10° denote "head-to-head" orientation, while those where T_1 lies between 170°-180° correspond to "head-to-tail" orientation of the 2,2′-bpy units (Scheme 3). Inspection of the corresponding torsion angles for the closest 2,2′-bpy units in **2cI** (T_1 = 43.75°) and **3** (T_1 = 72.65°) indicates that these rings do not overlap in "head-to-head" or "head-to-tail" fashion (Scheme 3), but rather in an in-between manner.

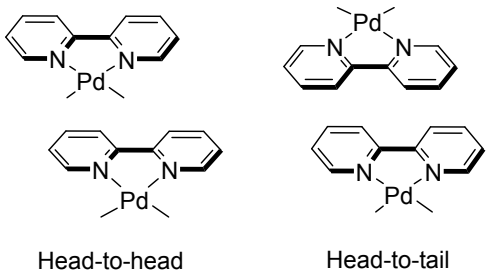

Scheme 3. Relative orientations of interacting 2,2′-bpy units in the crystals of various complexes. (Adapted from reference 35, reprinted with permission from Petrovic, P. V.; Janjic, G. V.; Zaric, S. D. Stacking Interactions between Square-Planar Metal Complexes with 2,2′-Bipyridine Ligands. Analysis of Crystal Structures and Quantum Chemical Calculations. *Cryst. Growth Des*. **2014**, *14*, 3880-3889. © 2014 American Chemical Society).

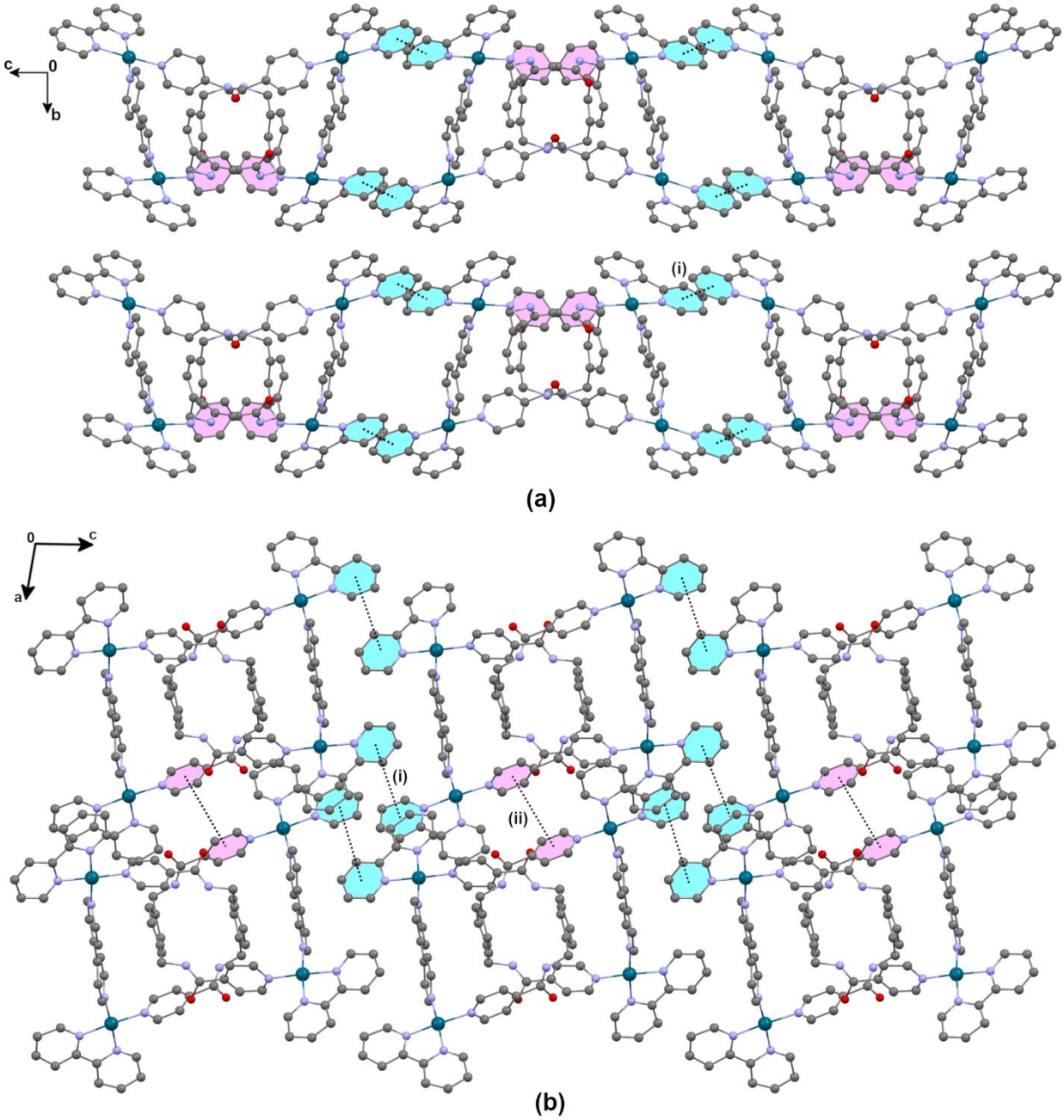

Figure 8. Views of the packing in crystals of **2cI** show (a) chain of [2]catenanes along the *c* axis linked *via* π…π interactions between bpy units [(i) Cg4···Cg7, Table S4] and (b) weak π…π interactions [(ii) Cg5···Cg5, Table S4] between the chains along the *a*-axis. Hydrogen atoms are omitted for clarity.

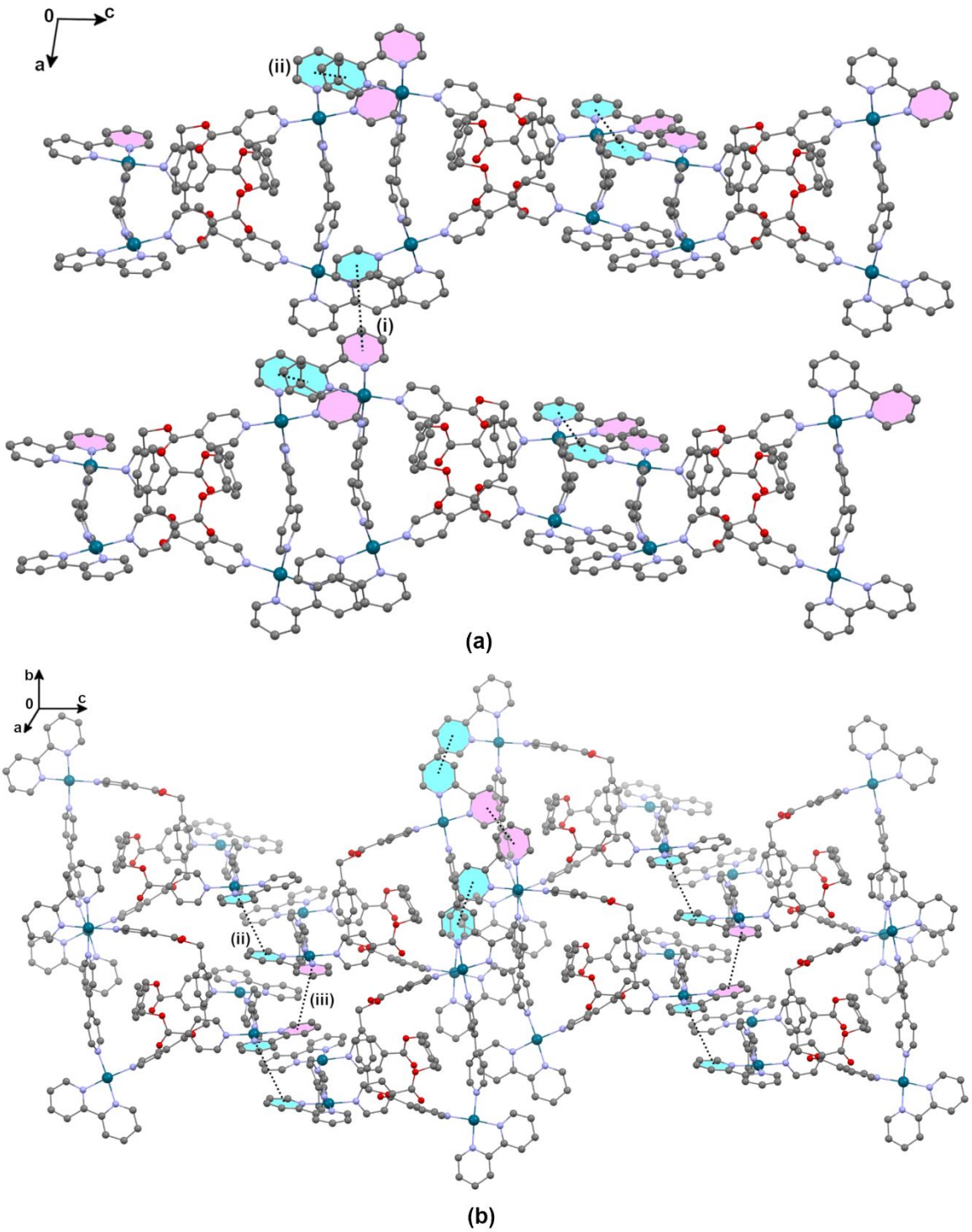

Figure 9. Views of the packing in crystals of **3** show (a) chain of [2]catenanes formed by π…π interactions between bpy units [(i) Cg4···Cg7 along *a*-axis and (ii) Cg8···Cg19 along *c*-axis, Table S4] and (b) weak π…π interactions [(iii) Cg7···Cg18, Table S4] between the chains along the *b*-axis. Hydrogen atoms, anions and water molecules are omitted for clarity.

This is perhaps due to the awkward shape of the molecule and the need to achieve efficiency in molecular packing, utilizing the aromatic surfaces of the bpy rings. Interestingly, the tetranuclear Pd(II) based molecular squares SERWEU and SERWIY reported by us earlier, also exhibit molecular packing through π…π stacking interactions between 2,2′-bpy units.[34] A striking difference in the molecular packing in the solvatomorphs SERWEU and SERWIY is the "head-to-tail" orientation of the interacting 2,2′-bpy units in SERWEU, unlike the weak overlap of these units in SERWIY (Figure 10). This change is perhaps due to the presence of a guest (acetic acid) and tosylate anions in SERWIY which influence the molecular organization of the squares.

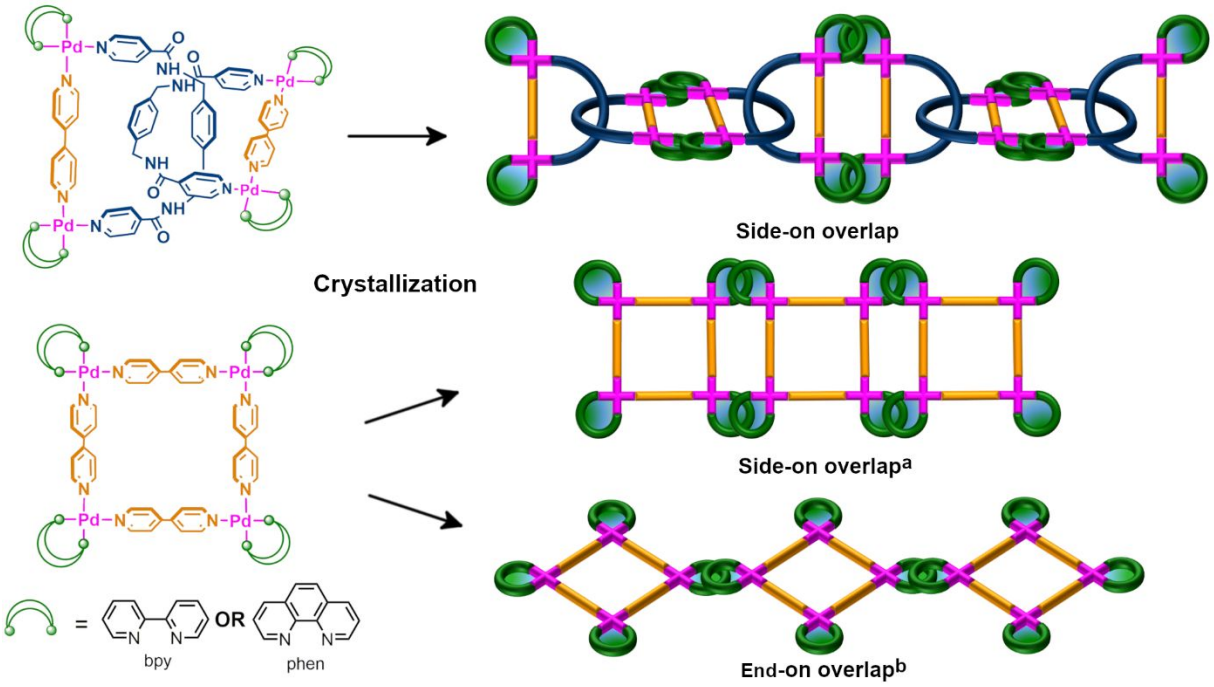

Figure 10. Schematic representation of the molecular association via side-on and end-on overlap modes in two different tetranuclear Pd(II) complexes. [a]Structure SERWIY[8]; [b]Structures SERWEU, SERWOE, SERWUK.[8] (Adapted from reference 34, reprinted with permission from Krishnaswamy, S.; Prusty, S.; Chartrand, D.; Hanan, G. S.; Chand, D. K. Self-Assembled Molecular Squares as Supramolecular Tectons. *Cryst. Growth Des.* **2018**, *18*, 2016-2030. © 2018 American Chemical Society).

Similar modes of molecular assembly are observed in the crystals of **2cI** (Figure 8a) and **2dI** (Figure S81a). The replacement of bpy with phen as the *cis*-protecting agent for the Pd(II) center often yields isostructural crystals.[34,41-44] However, the π…π stacking interactions between the closest phenanthroline units in **2dI** that link the catenanes across the *c*-axis are marginally shorter (~3.7-4.1 Å, Table S4) than those between the bpy units in **2cI**, possibly due to the better overlap between the aromatic rings of the phen moieties as compared to those of bpy. The second significant difference is the presence of π stacking interactions (~3.7-4.1 Å) between phen units which help in linking the chains along the *b*-axis. The chains are linked along the *a*-axis by C=O···π interactions between the amide carbonyl group and the one of the rings of a neighboring phen unit (Figure S81b).

In the crystals of **2dII** (Figure 11a) the π…π stacking interactions (Table S4) that connect the catenanes along the *c*-axis are shorter (~3.5-3.7 Å) than those in **2cI**, **2dI** and **3**. The chains are also linked along the *b*-axis by stacking interactions of phen units and along the *a*-axis by weak stacking interactions (~4.3 Å) between the pyridine rings of the ligands. Therefore, the solvatomorphs show slight differences in the modes of molecular packing in the crystal and the strength of the π stacking interactions.

The torsion angles for the closely interacting phen units in **2dI** ($T_1 = 42.62°$) and **2dII** ($T_1 = 46.40°$, 29.05°) indicate that these rings do not overlap in "head-to-head" or "head-to-tail" fashion but in an in-between manner similar to that observed in **2cI** and **3**. It is pertinent to note that the Pd(II) molecular squares SERWOE[34] and SERWUK[34] exhibited "head-to-tail" overlap of the interacting phen units in their crystals possibly due to the nearly coplanar nature of the Pd(II) square planes (Figure 10). While the importance of an aqueous medium for the formation of these [2]catenanes is now well understood, the crystal structures of these interlocked molecules (**2dII** and **3**) also

revealed the presence of a large number of water molecules which are involved in extensive hydrogen bonding interactions with the nitrate counteranions (FigureS82).

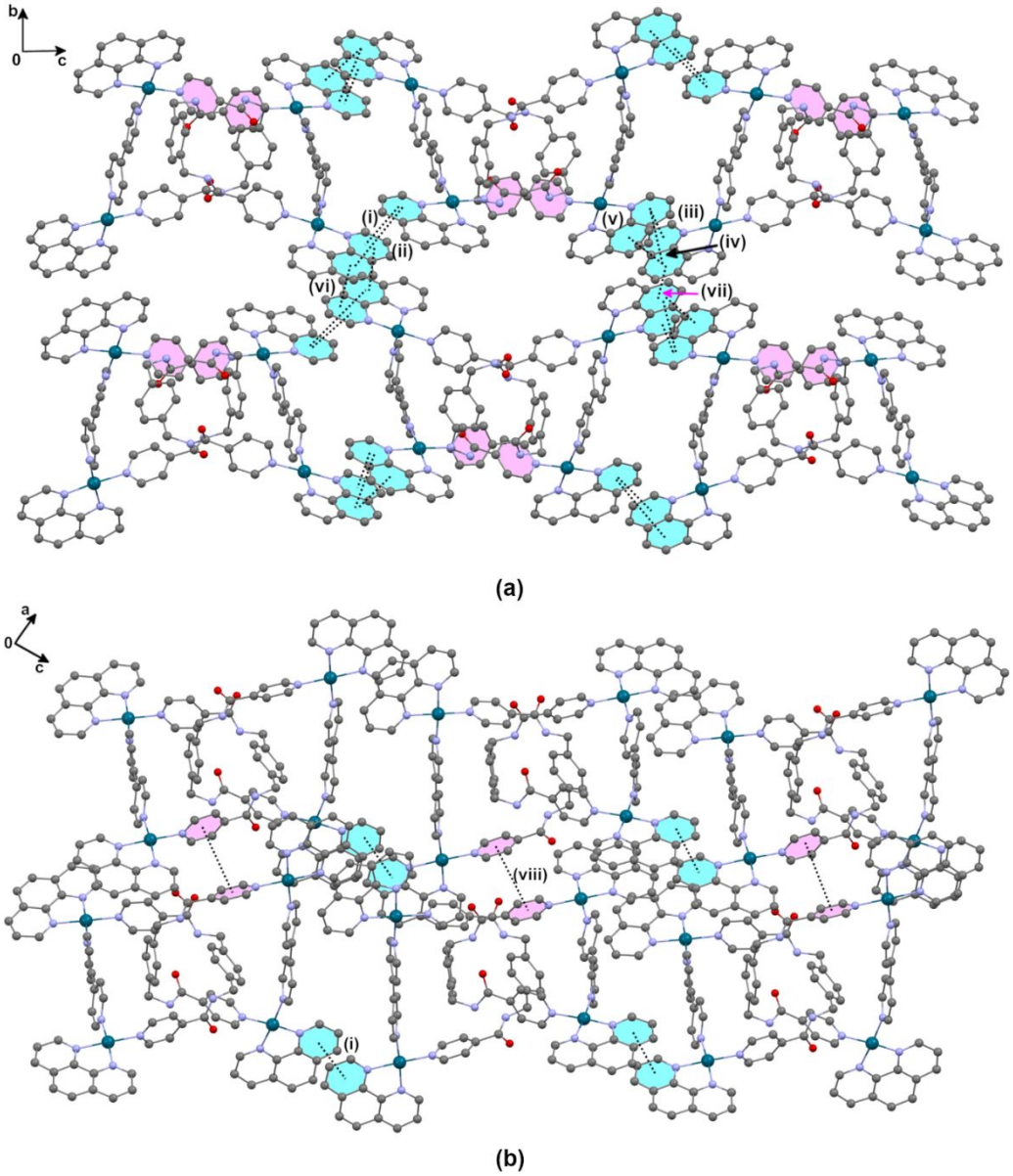

Figure 11. Views of the packing in crystals of **2dII** show (a) chain of [2]catenanes along the *c* axis linked *via* π…π interactions between phen units [see Table S4 for details of (i)-(vii)] and (b) weak π…π interactions [(viii) Cg12···Cg26, Table S4] between the chains in the *ac*-plane. Hydrogen atoms, anions and water molecules are omitted for clarity.

EXPERIMENTAL SECTION

4,4′-Bipyridine, $PdCl_2$ and silver salts were acquired from Aldrich Chemicals. The *cis*-protected Pd(II) units used were synthesized using reported procedures.[45,46] The compounds represented by Pd(**L′**)$(BF_4)_2$ were prepared by reacting Pd**(L′)**Cl_2 with $AgBF_4$. Ligand **L1** was prepared using a reported procedure.[36] All common reagents and solvents were obtained from Spectrochem, India. Deuterated solvents were obtained from Aldrich and Cambridge Isotope Laboratories. NMR spectra were recorded on Bruker 400 and 500 MHz FT-NMR spectrometers using tetramethylsilane as reference. Diffusion Ordered Spectroscopy (DOSY) NMR measurements were performed on a Bruker Avance (AV III) 500 MHz NMR spectrometer, equipped with a 5-mm broadband observe (BBO) z-axis gradient probe which delivers a maximum gradient strength of 50 G/cm. The mass spectra were recorded using a Bruker ESI-TOF/ESI-TRAP/FTMS fitted with a Bruker Cryospray system. Melting points were determined using a CINTEX apparatus and were uncorrected. Single crystal X-ray diffraction data were recorded on a Bruker AXS Kappa Apex II CCD diffractometer with graphite-monochromatized Mo-Kα (λ=0.71073 Å) radiation and a Bruker Venture Metaljet diffractometer equipped with an Oxford Cryosystem liquid nitrogen device, using Ga-Kα radiation (λ = 1.34180 Å).

Synthesis of ligand L1. To a stirred suspension of isonicotinoyl chloride hydrochloride (0.57 g, 3.23 mmol) and 1,4-phenylenedimethanamine (0.20 g, 1.46 mmol) in dry dichloromethane (25 mL), triethylamine (0.5 mL) was added in a dropwise manner at 0-5 °C. The mixture was stirred at room temperature for 24 h under nitrogen atmosphere. The solid obtained was filtered and washed repeatedly with distilled water, followed by diethyl ether and dried under vacuum, yielding a white solid. Isolated yield = 0.436 g, 86%, mp. 202 °C.

^{1}H NMR (500 MHz, DMSO-d_6, 298 K): δ [ppm] = 9.85 (t, J = 5.8 Hz, 2H, -N*H*-), 9.25 (d, J = 6 Hz, 4H, *H*a), 8.31 (d, J = 6 Hz, 4H, *H*b), 7.8 (s, 4H, *H*d), 5.01 (d, J = 5.9 Hz, 4H, *H*c).

General procedure A: Synthesis of the complexes 1a-d. Ligand **L1.** (0.005 mmol), **L2** (0.005 mmol), and the corresponding *cis*-protected Pd(II) unit (2 equiv.) were taken in DMSO or DMF (3 mL) and stirred for 24 h at ambient temperature to obtain a clear yellow solution. In a typical isolation process, addition of excess EtOAc gave an off-white precipitate which was separated by filtration, washed several times with EtOAc and dried under vacuum to obtain an off-white solid. All complexes were isolated by the same method.

$[Pd_2(en)_2(\mathbf{L1})(\mathbf{L2})](NO_3)_4$, **1a**: The complex was synthesized according to general procedure A (in DMF) using **L1** (1.7 mg, 0.005 mmol, 1 equiv), **L2** (0.8 mg, 0.005 mmol, 1 equiv), and $Pd(en)(NO_3)_2$ (3.0 mg, 0.010 mmol, 2 equiv). Isolated yield = 4.15 mg, mp. 230 °C (decomposed). ^{1}H NMR (500 MHz, DMSO-d_6) δ [ppm] = 9.89 (t, J = 5.7 Hz, 2H, -N*H*-), 9.47 (t, 8H, *H*a+*H*e), 8.60 and 8.39 (d and d, J = 6.5 and 6.5 Hz, 4H and 4H, *H*b and *H*f), 7.73 (s, 4H, *H*d), 6.23 and 6.19 (s and s, 4H and 4H, Hg_1, and Hg_2), 4.90 (d, J = 5.6 Hz, 4H, *H*c), 3.23 (s, 8H, *H*h).

^{13}C NMR (125 MHz, DMSO-d_6): δ [ppm] = 162.72, 152.81, 152.75, 145.42, 144.32, 138.27, 128.86, 127.92, 124.21. 47.32, 46.37, 43.17.

MS (CSI): *m/z* calcd for $[\mathbf{1a}\text{-}2NO_3]^{2+}$: 480.0663; found: 480.0674.

$Pd_2(tmeda)_2(\mathbf{L1})(\mathbf{L2})](NO_3)_4$, **1b**: The complex was synthesized according to general procedure A (in DMF) using **L1** (1.8 mg, 0.005 mmol, 1 equiv), **L2** (0.8 mg, 0.005 mmol, 1 equiv), and $Pd(tmeda)(NO_3)_2$ (3.5 mg, 0.010 mmol, 2 equiv). Isolated yield = 4.80 mg, mp. 242 °C (decomposed).

^{1}H NMR (500 MHz, DMSO-d_6) δ [ppm] = 9.93 (t, J = 5.95 Hz, 2H, -N*H*-), 9.77 (t, 8H, *H*a+*H*e), 8.70 and 8.50 (d and d, J = 5.45 and 6.05 Hz , 4H and 4H, *H*b+*H*f), 7.73 (s, 4H, *H*d), 4.89 (d, J = 5.6 Hz, 4H, *H*c), 3.53 (s, 8H, *H*j), 3.13 and 3.11 (s and s, 12H and 12H, Hi_1+Hi_2).

^{13}C NMR (125 MHz, DMSO-d_6) δ [ppm] = 162.48, 152.36, 145.09, 144.12, 138.59, 129.14, 125.09, 124.90, 62.89, 51.02, 50.97, 43.39.

MS (CSI): *m/z* calcd for [1**b**-2NO_3]$^{2+}$: 536.1291, found: 536.1309.

[Pd_2(bpy)$_2$(**L1**)(**L2**)](NO_3)$_4$, **1c**: The complex was synthesized according to general procedure A (in DMSO or DMF) using **L1** (1.8 mg, 0.005 mmol, 1 equiv), **L2** (0.8 mg, 0.005 mmol, 1 equiv), and Pd(bpy)(NO_3)$_2$ (4.0 mg, 0.010 mmol, 2 equiv). Isolated yield = 5.45 mg, mp. 222 °C (decomposed).

^{1}H NMR (500 MHz, DMSO-d_6) δ [ppm] = 10.05 (t, J = 5.8 Hz, 2H, -N*H*-), 9.89 and 9.86 (d and d, J = 5.8 and 5.5 Hz, 4H and 4H *H*a+*H*e), 9.33 (d, J = 8.2 Hz, 4H, *H*n), 9.03-9.08 (m, 4H, Hm_1+Hm_2), 8.82 and 8.61(d and d, J = 5.9 and 6.6 Hz, 4H and 4H, *H*b+*H*f), 8.21-8.35 (m, 4H and 4H, Hk_1+Hk_2 and Hl_1+Hl_2), 7.78 (s, 4H, *H*d), 4.94 (d, J = 5.8 Hz, 4H, *H*c).

^{13}C NMR (125 MHz, DMSO-d_6): δ [ppm] = 162.26, 156.23, 152.49, 152.41, 151.16, 145.86, 144.63, 143.29, 138.41, 129.14, 129.03, 125.61, 125.56, 125.10, 43.25.

MS (CSI): *m/z* calcd for [**1c**-3NO_3]$^{3+}$: 363.3816; found: 363.3857.

[Pd_2(phen)$_2$(**L1**)(**L2**)](NO_3)$_4$, **1d**: The complex was synthesized according to general procedure A (in DMSO or DMF) using **L1** (1.8 mg, 0.005 mmol, 1 equiv), **L2** (0.8 mg, 0.005 mmol, 1 equiv), and Pd(phen)(NO_3)$_2$ (4.2 mg, 0.010 mmol, 2 equiv). Isolated yield = 5.90 mg, mp. 236 °C (decomposed).

^{1}H NMR (500 MHz, DMSO-d_6) δ [ppm] = 10.07 (t, J = 5.9 Hz, 2H, -N*H*-), 9.97 and 9.94 (d and d, J = 5.3 and 5.1 Hz, 4H and 4H, *H*a and *H*e), 9.68-9.72 (m, 4H, Hq_1 and Hq_2), 9.00 (s, 4H, *H*r),

8.88 and 8.66 (d and d, J = 5.4 and 6.6 Hz, 4H and 4H, *H*b and *H*f), 8.83 and 8.70 (d and d, J = 5.2 and 5.1 Hz, 2H and 2H, Ho_1 and Ho_2), 8.62 and 8.58 (dd and dd, J = 8.2, 5.3 and 8.3, 5.3 Hz, 2H and 2H, Hp_1 and Hp_2), 7.81 (s, 4H, *H*d), 4.97 (d, J = 5.8 Hz, 4H, *H*c).

^{13}C NMR (125 MHz, DMSO-d_6): δ [ppm] = 162.36, 152.85, 152.73, 152.24, 146.38, 146.03, 144.78, 142.10, 138.48, 131.10, 129.08, 128.71, 127.44, 125.67, 43.31.

MS (CSI): *m/z* calcd for [**1d**-3NO_3]$^{3+}$: 379.3817, found: 379.3842.

General procedure B Synthesis of equilibrium mixture of complexes 1a-d and 2a-d). Ligand **L1** (0.025 mmol), **L2** (0.025 mmol), and the corresponding *cis*-protected Pd(II) unit (0.050 mmol) were mixed in 5 mL water and stirred for 24 h at ambient temperature to obtain a clear solution, which, upon slow evaporation yielded a pale yellow solid/crystals. The solid upon dissolution in D_2O, revealed two sets of signals corresponding to the macrocycle (**1a-d**) and [2]catenane (**2a-d**), respectively.

$[Pd_2(en)_2(\mathbf{L1})(\mathbf{L2})](NO_3)_4$, **1a** and $[Pd_4(en)_4(\mathbf{L1})_2(\mathbf{L2})_2](NO_3)_8$, **2a**: The equilibrium mixture was synthesized according to general procedure B using **L1** (8.6 mg, 0.025 mmol, 1 equiv) **L2** (3.9 mg, 0.025 mmol, 1 equiv), and $Pd(en)(NO_3)_2$ (14.5 mg, 0.050 mmol, 2 equiv). Isolated yield = 25.6 mg.

1a: ^{1}H NMR (500 MHz, D_2O): δ [ppm] = 8.83 and 8.81(d and d, J = 6.75 and 6.8 Hz, 4H and 4H, *H*a and *H*e), 7.81 and 7.79 (d and d, J = 6.85 and 6.75 Hz, 4H and 4H, *H*b and *H*f), 7.19 (s, 4H, *H*d), 4.53 (s, 4H, *H*c), 2.93 (s, 24H, *H*h and *H*h′).

2a: ^{1}H NMR (500 MHz, D_2O): δ [ppm] = 9.11 and 8.92 (d and d, J = 6.8 and 6.75 Hz, 8H and 8H, *H*a′ and *H*e′), 7.96 and 7.66 (d and d, J = 6.85 and 6.8 Hz, 8H and 8H, *H*b′ and *H*f′), 4.82 (s, 8H, *H*d′), 3.73 (s, 8H, *H*c′), 2.93 (s, 24H, *H*h and *H*h′).

1a/**2a**: ^{13}C NMR (125 MHz, D_2O): δ [ppm] = 164.44, 152.45, 152.11, 145.42, 144.21, 135.38, 127.05, 124.87, 124.75, 124.57, 124.14, 47.03, 42.64.

$[Pd_2(tmeda)_2(\mathbf{L1})(\mathbf{L2})](NO_3)_4$, **1b** and $[Pd_4(tmeda)_4(\mathbf{L1})_2(\mathbf{L2})_2](NO_3)_8$, **2b**: The equilibrium mixture was synthesized according to general procedure B using **L1** (8.6 mg, 0.025 mmol, 1 equiv) **L2** (3.9 mg, 0.025 mmol, 1 equiv), and $Pd(tmeda)(NO_3)_2$ (17.3 mg, 0.050 mmol, 2 equiv). Isolated yield = 26.20 mg.

1b: ^{1}H NMR (500 MHz, D_2O): δ [ppm] = 9.14 and 9.07 (d and d, J = 5.45 and 5.60 Hz, 4H and 4H, *H*a and *H*e), 7.92 and 7.89 (d and d, J = 5.55 and 5.35 Hz, 4H and 4H, *H*b and *H*f), 7.16 (s, 4H, *H*d), 4.52 (s, 4H, *H*c), 3.14 (s, 8H, *H*j), 2.72 and 2.69 (s and s, 12H and 12H, Hi_1+Hi_2).

2b: ^{1}H NMR (500 MHz, D_2O): δ [ppm] = 9.33 and 9.10 (d and d, J = 5.55 and 5.60 Hz, 8H and 8H, *H*a′ and *H*e′), 8.15 and 7.83 (d and d, J = 5.50 and 5.65 Hz, 8H and 8H, *H*b′ and *H*f′), 4.76 (s, 8H, *H*d′), 3.76 (s, 8H, *H*c′), 3.14 (s, 16H, *H*j′), 2.75 and 2.66 (s and s, 24H and 24H, Hi_1'+Hi_2').

1b/**2b**: ^{13}C NMR (125 MHz, D_2O): δ = 163.79, 152.21, 151.81, 144.67, 144.56, 135.38, 127.21, 125.72, 124.36, 63.01, 50.60, 50.52, 42.71.

The mixture of **1b′** and **2b′** was prepared in a similar manner by using $Pd(tmeda)(BF_4)_2$ instead of $Pd(tmeda)(NO_3)_2$. MS (CSI): *m/z* calcd for $[\mathbf{1b'}\text{-}3(BF_4)]^{3+}$: 776.5281; found 776.5318 and *m/z* calcd for $[\mathbf{2b'}\text{-}2(BF_4)]^{2+}$: 560.6452; found: 560.6462.

$[Pd_2(bpy)_2(\mathbf{L1})(\mathbf{L2})](NO_3)_4$, **1c** and $[Pd_4(bpy)_4(\mathbf{L1})_2(\mathbf{L2})_2](NO_3)_8$, **2c**: The equilibrium mixture was synthesized according to general procedure B using **L1** (8.6 mg, 0.025 mmol, 1 equiv), **L2** (3.9 mg, 0.025 mmol, 1 equiv), and $Pd(bpy)(NO_3)_2$ (19.3 mg, 0.050 mmol, 2 equiv). Isolated yield = 27.20 mg.

1c: ^{1}H NMR (400 MHz, D_2O): δ [ppm] = 9.28 and 9.25 (d and d, J = 6.6 and 6.6 Hz, 4H and 4H, *H*a and *H*e), 8.51-8.57 (m, 12H, *H*n+*H*n′), 8.39-8.50 (m, 12H, Hm_1+ Hm_2+Hm_1′+Hm_2′), 8.13 and

8.06 (d and d, J = 6.6 and 6.8 Hz, 4H and 4H, *H*b and *H*f), 7.58-7.82 (m, 24H, *H*k_1+*H*k_2+ *H*k_1' +*H*k_2'+*H*l_1+*H*l_2+*H*l_1'+*H*l_2'), 7.28 (s, 4H, *H*d) and 4.63 (s, 4H, *H*c).

2c: ^{1}H NMR (400 MHz, D_2O): δ [ppm] = 9.53 and 9.34 (d and d, J = 6.7 and 6.7, 8H and 8H, *H*a′ and *H*e′), 8.51-8.57 (m, 12H, *H*n+*H*n′), 8.39-8.50 (m, 12H, *H*m_1+ *H*m_2+*H*m_1'+*H*m_2'), 8.32 and 8.03 (d and d, J = 6.7 and 6.8 Hz, 8H and 8H, *H*b′ and *H*f′), 7.58-7.82 (m, 24H, *H*k_1+*H*k_2+ *H*k_1' +*H*k_2'+*H*l_1+*H*l_2+*H*l_1'+*H*l_2'), 5.03 (s, 8H, *H*d′), and 3.92 (s, 8H, *H*c′).

1c/**2c**: ^{13}C NMR (125 MHz, D_2O): δ [ppm] = 165.48, 164.04, 156.86, 152.65, 152.33, 152.20, 150.45, 150.31, 150.16, 147.12, 145.73, 142.99, 136.89, 135.55, 128.26, 127.80, 127.39, 126.14, 125.83, 125.69, 125.24, 124.62, 124.55, 43.39, and 42.84.

The mixture **1c′/2c′** was prepared in a similar manner by using Pd(bpy)$(BF_4)_2$ instead of Pd(bpy)$(NO_3)_2$. MS (CSI): *m/z* calcd for [**1c′**-3(BF_4)]$^{3+}$: 829.7782; found: 829.7838 and *m/z* calcd for [**2c′**-2(BF_4)]$^{2+}$: 600.5827; found: 600.5831.

[Pd_2(phen)$_2$(**L1**)(**L2**)]$(NO_3)_4$, **1d** and [Pd_4(phen)$_4$(**L1**)$_2$(**L2**)$_2$]$(NO_3)_8$, **2d**: The equilibrium mixture was synthesized according to general procedure B using **L1** (8.6 mg, 0.025 mmol, 1 equiv), **L2** (3.9 mg, 0.025 mmol, 1 equiv), and Pd(phen)$(NO_3)_2$ (20.5 mg, 0.050 mmol, 2 equiv). Isolated yield = 28.5 mg.

1d: ^{1}H NMR (400 MHz, D_2O): δ [ppm] = 9.38 and 9.36 (d and d, J = 6.6 and 6.4 Hz, 4H and 4H, *H*a and *H*e), 8.98-9.05 (m, 12H, *H*q_1+*H*q_2+*H*q_1'+*H*q_2'), 8.33 (s, 12H, *H*r+*H*r′), 8.21 (d, J = 6.7 Hz, 4H, *H*b/*H*f), 8.19-8.08 (m, 16H, *H*b/*H*f+*H*o_1+*H*o_2+*H*o_1'+*H*o_2'), 8.06-7.93 (m, 12H, *H*p_1+*H*p_2+*H*p_1'+*H*p_2'), 7.31 (s, 4H, *H*d), 4.66 (s, 4H, *H*c).

2d: ^{1}H NMR (400 MHz, D_2O): δ [ppm] = 9.63 and 9.46 (d and d, J = 6.4 and 6.5 Hz, 8H and 8H, *H*a′ and *H*e′), 8.98-9.05 (m, 12H, *H*q_1+*H*q_2+*H*q_1'+*H*q_2'), 8.37 (d, 4H, J = 6.5 Hz, *H*b′/*H*f′) and 8.12 (d, 4H, *H*b′/*H*f′ merged with *H*b/*H*f), 8.33 (s, 12H, *H*r_1+*H*r_2+*H*r_1'+*H*r_2'), 8.19-8.08 (m, 16H,

*H*b/*H*f+*H*o$_1$+*H*o$_2$+*H*o$_1$′+*H*o$_2$′), 8.06-7.93 (m, 12H, *H*p$_1$+*H*p$_2$+*H*p$_1$′+*H*p$_2$′), 5.12 (s, 8H, *H*d′), 3.99 (s, 8H, *H*c′).

1d/**2d**: ^{13}C NMR (125 MHz, D_2O): δ [ppm] = 152.90, 152.59, 152.47, 150.95, 147.26, 142.10, 141.97, 136.90, 131.47, 131.42, 128.33, 127.82, 127.40, 126.30, 126.16, 125.89, 125.70, 125.31, 43.40.

The mixture **1d′/2d′** was prepared in a similar manner by using Pd(phen)$(BF_4)_2$ instead of Pd(phen)$(NO_3)_2$. MS (CSI): *m/z* calcd for [**1d′**-3(BF_4)]$^{3+}$: 861.7783; found: 861.7873 and *m/z* calcd for [**2d′**-(BF4)]$^{1+}$: 1336.1696; found: 1336.1727.

Crystallographic details. The crystals of [2]catenanes **2cI**, **2dI** and **2dII** were less stable as compared to those of **3** and rapidly lost crystallinity when exposed to air. Single-crystal X-ray measurements were recorded for crystals of **2cI** and **2dI** (by mounting the crystal on the goniometer head using a Lindemann capillary) on a Bruker AXS Kappa Apex II CCD diffractometer with graphite-monochromatized Mo-Kα (λ=0.71073 Å) radiation. The automatic cell determination routine, with 36 frames at three different orientations of the detector, was employed to collect reflections, and the APEXII-SAINT program[47] was used for determining the unit cell parameters. The data were corrected for Lorentz-polarization effects. Semi-empirical absorption correction (multi-scan) based on symmetry equivalent reflections was applied using the SADABS program.[47] The structures were solved by direct methods and refined by full matrix least squares, based on F^2 using SHELX-2014 software package[48] and the program WinGX.[49] Molecular and packing diagrams were generated using Mercury.[50] Geometrical calculations were performed using PLATON.[39] ORTEPs were prepared using ORTEP-3.[49] For **2dII** the X-ray measurements were performed on a single crystal mounted using a fibre loop on a Bruker Venture Metaljet diffractometer equipped with an Oxford Cryosystem liquid N2 device, using Ga-Kα

radiation (λ = 1.34180 Å). The cell parameters were determined from reflections taken from three sets of 100 frames. The structure was solved by direct methods using SHELX-2014 software package and the program Olex2.[51] The crystallographic data for the crystals of **2cI, 2dI** and **2dII** are summarized in Table 1. Details regarding the refinement of the structures are available in the Supporting Information.

CONCLUSIONS

A series of concentration dependent equilibrium mixtures of [2]catenanes and the corresponding macrocycles were synthesized using a flexible pyridine-appended ligand, 4,4′-bipyridine and *cis*-protected Pd(II) units. Two concomitant crystalline forms were obtained in the case of the [2]catenane containing phenanthroline moieties in the *cis*-protected Pd(II) units. These dimorphs show subtle differences in the orientation of the amide carbonyl groups and *cis*-protected Pd(II) units and the strength of the π…π stacking interactions in their structures. The aromatic rings of the adjacent 1,10-phenanthroline units exhibit stronger interactions as compared to those of the 2,2′-bpy units, due to the presence of an additional ring which allows for better overlap. A possible route for the formation of the [2]catenane consists of two steps: dissociation of the coordinate bond between the ligand and the Pd(II) center of one macrocycle, allowing for quick threading of the second macrocycle followed by closure of the former ring.[33] During these reversible processes, differences in the relative orientation of the two rings and conformational changes in the structures of the ring components result in conformational isomerism. These conformational isomers can crystallize and yield solvatomorphs which exhibit differences in the orientation of functional groups and ring components in the solid state giving rise to conformational solvatomorphism in these mechanically interlocked molecules.

ASSOCIATED CONTENT

Supporting Information

1D and 2D NMR spectra for complexes **1a-d** in DMSO-d_6, 1D and 2D NMR spectra for mixtures **1a**/**2a**, **1b**/**2b**, **1c**/**2c** and **1d**/**2d** in D_2O, 1D and 2D NMR spectra for **2a-d** in D_2O (higher concentrations), 2D DOSY NMR spectra for **1a**/**2a**, **1b**/**2b**, **1c**/**2c** and **1d**/**2d**, ^{1}H NMR spectra for **1a**/**2a**, **1b**/**2b**, **1c**/**2c** and **1d**/**2d** at different concentrations, plot of percentage of rings in the catenane and macrocycle versus concentration, table of equilibrium constants calculated for **1a**/**2a**, **1b**/**2b**, **1c**/**2c** and **1d**/**2d** at different concentrations, CSI-MS data for **1a-d** (DMSO), CSI-MS data for **1b′/2b′**, **1c′/2c′**, **1d′/2d′** (D_2O), crystallographic data table, details of crystal structure solution, ORTEPs of **2cI**, **2dI** and **2dII**, molecular packing diagram for **2dI**, chemical structure of **3**, table of intermolecular interactions in crystals of **2cI**, **2dI**, **2dII** and **3**.

Accession codes

CCDC 1988795-1988797 contain the supplementary crystallographic data for this paper. These data can be obtained free of charge via www.ccdc.cam.ac.uk/data_request/cif, or by emailing data_request@ccdc.cam.ac.uk, or by contacting The Cambridge Crystallographic Data Centre, 12 Union Road, Cambridge CB2 1EZ, UK; fax: +44 1223 336033.

AUTHOR INFORMATION

Corresponding Author

Dillip K. Chand - Department of Chemistry, Indian Institute of Technology Madras, Chennai 600 036, India; ORCID: 0000-0003-1115-0138; Email: dillip@iitm.ac.in

Authors

Shobhana Krishnaswamy- Department of Chemistry, Indian Institute of Technology Madras, Chennai 600 036, India; ORCID: 0000-0003-2479-2826

Soumyakanta Prusty- Department of Chemistry, Indian Institute of Technology Madras, Chennai 600 036, India; ORCID: 0000-0002-7525-5716

Daniel Chartrand- Department of Chemistry, University of Montreal, Montreal QC H3T-IJ4 (Canada) ORCID: 0000-0003-0851-7701

Garry S. Hanan- Department of Chemistry, University of Montreal, Montreal QC H3T-IJ4 (Canada); ORCID: 0000-0001-6671-5234

ACKNOWLEDGEMENTS

D.K.C. thanks Science and Engineering Research Board (SERB), the Department of Science and Technology, Govt. of India (Project No. EMR/2017/002262) for financial support. S.K. thanks IIT-Madras for an Institute Postdoctoral Fellowship and S.P. thanks C.S.I.R., India for a research fellowship. G.S.H. and D.C. thank the Natural Sciences and Engineering Research Council (NSERC) of Canada for financial support. We thank Dr. Babu Varghese and Dr. B. Chandrika (S.A.I.F., IIT Madras) for their help with collecting X-ray diffraction data and 2D-DOSY NMR experiments, respectively.

REFERENCES

1. Bernstein, J. *Polymorphism in Molecular Crystals*, Oxford University Press, Oxford, UK, 2002.
2. Sarma, J. A. R. P.; Desiraju, G. R. *Crystal Engineering: Polymorphism and Pseudopolymorphism in Organic Crystals: A Cambridge Structural Database Study*, ed. Seddon, S. R. and Zaworotko, M. Kluwer, Norwell, MA, USA, 1999.
3. Shashidhar, M. S.; Krishnaswamy, S. Intermolecular Acyl-Transfer Reactions in Molecular Crystals. *Acc. Chem. Res*. **2019**, *52*, 437-446.
4. Cruz-Cabeza, A. J.; Bernstein, J. Conformational Polymorphism. *Chem. Rev.* **2014**, *114*, 2170-2191.
5. Nangia, A. Conformational Polymorphism in Organic Crystals. *Acc. Chem. Res.* **2008**, *41*, 595-604.
6. Brittain, H. G. *Polymorphism in Pharmaceutical Solids*, *Second Edition*, CRC Press, New York, 2016.
7. Rohani, S.; Lu, J. Polymorphism and Crystallization of Active Pharmaceutical Ingredients (APIs). *Curr. Med. Chem.* **2009**, *16*, 884-905.
8. Groom, C. R.; Bruno, I. J.; Lightfoot, M. P.; Ward, S. C. The Cambridge Structural Database. *Acta Crystallogr., Sect. B: Struct. Sci., Cryst. Eng. Mater.* **2016**, *72*, 171-179.
9. Cruz-Cabeza, A. J.; Reutzel-Edens, S. M.; Bernstein, J. Facts and fictions about polymorphism. *Chem. Soc. Rev*. **2015**, *44*, 8619-8635.
10. Orlando, T.; Salbego, P. R. S.; Taschetto, C. L. R.; Bonacorso, H. G.; Zanatta, N.; Hoerner, M.; Martins, M. A. P. Polymorphism in a Rotaxane Molecule: Intra- and Intermolecular Understanding. *Cryst. Growth Des.* **2019**, *19*, 1021-1030.

11. Baumes, J. M.; Murgu, I.; Oliver, A.; Smith, B. D. Using the Rotaxane Mechanical Bond to Enhance Chemical Reactivity. *Org. Lett*. **2010**, 12, 4980-4983.

12. Mezei, G.; Kampf, J. W.; Pecoraro, V. L. Temperature-, molar ratio- and counterion-effects on the crystal growth of bipyridinium-bis(alkylcarboxylic acid)-crown ether pseudorotaxanes. *New J. Chem*. **2007**, 31, 439-446.

13. Forgan, R. S.; Gassensmith, J. J.; Cordes, D. B.; Boyle, M. M.; Hartlieb, K. J.; Friedman, D. C.; Slawin, A. M. Z.; Stoddart, J. F. Self-Assembly of a [2]Pseudorota[3]catenane in Water. *J. Am. Chem. Soc.* **2012**, *134*, 17007-17010.

14. Sluysmans, D.; Stoddart, J. F. The Burgeoning of Mechanically Interlocked Molecules in Chemistry. *Trends Chem.* **2019**, *1*, 185-197 and references cited therein.

15. Bruns, C. J.; Stoddart, J. F. *The Nature of the Mechanical Bond: From Molecules to Machines*; John Wiley & Sons, Inc., Hoboken, NJ, USA, 2016.

16. Gil-Ramirez, G.; Leigh, D. A.; Stephens, A. J. Catenanes: Fifty Years of Molecular Links. *Angew. Chem., Int. Ed*. **2015**, *54*, 6110-6150.

17. Erbas-Cakmak, S.; Leigh, D. A.; McTernan, C. T.; Nussbaumer, A. L. Artificial Molecular Machines. *Chem. Rev*. **2015**, *115*, 10081-10206.

18. Evans, N. H.; Beer, P. D. Progress in the synthesis and exploitation of catenanes since the Millennium. *Chem. Soc. Rev*. **2014**, *43*, 4658-4683.

19. *Catenanes, Rotaxanes, and Knots - A Journey Through the World of Molecular Topology*; Dietrich-Buchecker, C. O.; Sauvage, J.-P., Eds.; Wiley-VCH: Weinheim, Germany, 1999.

20. Schalley, C. A.; Weilandt, T.; Bruggemann, J.; and Vögtle, F. Hydrogen-Bond-Mediated Template Synthesis of Rotaxanes, Catenanes, and Knotanes. *Top. Curr. Chem.* **2004**, *248*, 141-200.

21. Kidd, T. J.; Leigh, D. A.; Wilson, A. J. Organic "Magic Rings": The Hydrogen Bond-Directed Assembly of Catenanes under Thermodynamic Control. *J. Am. Chem. Soc.* **1999**, *121*, 1599-1600.

22. Mercurio, J. M.; Caballero, A.; Cookson, J.; Beer, P. D. A halogen- and hydrogen-bonding [2]catenane for anion recognition and sensing. *RSC Adv.* **2015**, *5*, 9298-9306.

23. Gilday, L. C.; Beer, P. D. Halogen- and Hydrogen-Bonding Catenanes for Halide-Anion Recognition. *Chem. - Eur. J.* **2014**, *20*, 8379-8385.

24. Gilday, L. C.; Lang, T.; Caballero, A.; Costa, P. J.; Félix, V.; Beer, P. D. A Catenane Assembled through a Single Charge-Assisted Halogen Bond. *Anew. Chem., Int. Ed.* **2013**, *52*, 4356-4360.

25. Li, H.; Zhang, H.; Lammer, A. D.; Wang, M.; Li, X.; Lynch, V. M.; Sessler, J. L. Quantitative self-assembly of a purely organic three-dimensional catenane in water. *Nat. Chem.* **2015**, *7*, 1003-1008.

26. Fang, L.; Basu, S.; Sue, C.-H; Fahrenbach, A. C.; Stoddart, J. F. Syntheses and Dynamics of Donor-Acceptor [2]Catenanes in Water. *J. Am. Chem. Soc.* **2011**, *133*, 396-399.

27. Au-Yeung, H. Y.; Pantos, G. D.; Sanders, J. K. M. Dynamic combinatorial synthesis of a catenane based on donor–acceptor interactions in water. *Proc. Natl. Acad. Sci. U. S. A.* **2009**, *106*, 10466-10470.

28. Langton, M. J.; Beer, P. D. Nitrate anion templated synthesis of a [2]catenane for nitrate recognition in organic–aqueous solvent media. *Chem. Commun.* **2014**, *50*, 8124-8127.

29. Spence, G. T.; Beer, P. D. Expanding the Scope of the Anion Templated Synthesis of Interlocked Structures. *Acc. Chem. Res*. **2012**, *46*, 571-586 and references cited therein.

30. Gibbs-Hall, I. C.; Vermeulen, N. A.; Dale, E. J.; Henkelis, J. J.; Blackburn, A. K.; Barnes, J. C.; Stoddart, J. F. Catenation through a Combination of Radical Templation and Ring-Closing Metathesis. *J. Am. Chem. Soc.* **2015**, *137*, 15640-15643.

31. Barnes, J. C.; Fahrenbach, A. C.; Cao, D.; Dyar, S. M.; Frasconi, M.; Giesener, M. A.; Benítez, D.; Tkatchouk, E.; Chernyashevskyy, O.; Shin, W. H.; Li, H.; Sampath, S.; Stern, C. L.; Sarjeant, A. A.; Hartlieb, K. J.; Liu, Z. C.; Carmieli, R.; Botros, Y. Y.; Choi, J. W.; Slawin, A. M. Z.; Ketterson, J. B.; Wasielewski, M. R.; Goddard, W. A.; Stoddart, J. F. A Radically Configurable Six-State Compound. *Science*, **2013**, *339*, 429-433.

32. Lewis, J. E. M.; Beer, P. D.; Loeb, S. J.; Goldup, S. M. Metal ions in the synthesis of interlocked molecules and materials. *Chem. Soc. Rev*. **2017**, *46*, 2577-2591 and references cited therein.

33. Fujita, M. Self-Assembly of [2]Catenanes Containing Metals in Their Backbones. *Acc. Chem. Res.* **1999**, *32*, 53-61 and references cited therein.

34. Krishnaswamy, S.; Prusty, S.; Chartrand, D.; Hanan, G. S.; Chand, D. K. Self-Assembled Molecular Squares as Supramolecular Tectons. *Cryst. Growth Des.* **2018**, *18*, 2016-2030.

35. Petrovic, P. V.; Janjic, G. V.; Zaric, S. D. Stacking Interactions between Square-Planar Metal Complexes with 2,2′-Bipyridine Ligands. Analysis of Crystal Structures and Quantum Chemical Calculations. *Cryst. Growth Des*. **2014**, *14*, 3880-3889.

36. Sumby, C. J.; Hanton, L. R. Syntheses and studies of flexible amide ligands: a toolkit for studying metallo-supramolecular assemblies for anion binding. *Tetrahedron*, **2009**, *65*, 4681-4691.

37. Prusty, S.; Krishnaswamy, S.; Bandi, S.; Chandrika, B.; Luo, J.; McIndoe, J. S.; Hanan, G. S.; Chand, D. K. Reversible Mechanical Interlocking of D-Shaped Molecular Karabiners bearing Coordination-Bond Loaded Gates: Route to Self-Assembled [2]Catenanes. *Chem. - Eur. J*. **2015**, *21*, 15174-15187.

38. Fujita, M.; Aoyagi, M.; Ibukuro, F.; Ogura, K.; Yamaguchi, K. Made-to-Order Assembling of [2]Catenanes from Palladium(II)-Linked Rectangular Molecular Boxes. *J. Am. Chem. Soc*. **1998**, 120, 611-612.

39. Spek, A. L. Structure validation in chemical crystallography. *Acta Crystallogr., Sect. D: Biol. Crystallogr*. **2009**, *65*, 148-155.

40. Kruszynski, R.; Sierański, T. Can Stacking Interactions Exist Beyond the Commonly Accepted Limits? *Cryst. Growth Des*. **2016**, *16*, 587-595.

41. Krishnaswamy, S.; Chand, D. K. *cis*-Protected palladium(II) based binuclear complexes as tectons in crystal engineering and the imperative role of the *cis*-protecting agent. *CrystEngComm* **2017**, *19*, 5157-5172.

42. Dasary, H.; Jagan, R.; Chand, D. K. Octadecanuclear Gear Wheels by Self-Assembly of Self-Assembled "Double Saddle" - Type Coordination Entities: Molecular "Rangoli". *Chem. - Eur. J*. **2015**, *21*, 1499-1507.

43. Tripathy, D.; Ramkumar, V.; Chand, D. K. Toppled Molecular-Domino Sets by Self-Assembly of Self-assembly: The π-Polymers. *Cryst. Growth Des.* **2013**, *13*, 3763-3772.

44. Naranthatta, M. C.; Das, D.; Tripathy, D.; Sahoo, H. S.; Ramkumar, V.; Chand, D. K. Consequence of Presence and Absence of π-Clouds at Strategic Locations of Designed Binuclear Pd(II) Complexes on Packing: Self-Assembly of Self-Assembly by Intermolecular Locking and Packing. *Cryst. Growth Des.* **2012**, *12*, 6012-6022.

45. Wimmer, S.; Castan, P.; Wimmer, F. L.; Johnson, N. P. Preparation and Interconversion of Dimeric Di-μ-hydroxo and Tri-μ-hydroxo complexes of Platinum(II) and Palladium(II) with 2,2′-Bipyridine and 1,10-Phenanthroline. *J. Chem. Soc., Dalton Trans. (1972-1999)* **1989**, 403-412.

46. Drew, H. D. K.; Pinkard, F. W.; Preston, G. H.; Wardlaw, W. The Supposed Isomerism among the Palladodiammines. *J. Chem. Soc.* **1932**, 1895-1909.

47. *SADABS* (v 2.05), *SMART* (v 5.631), and *SAINT* (v 6.45); Bruker AXS Inc.; Madison, Wisconsin, USA, 2003.

48. Sheldrick, G. M. Crystal structure refinement with *SHELXL*. *Acta Crystallogr*., *Sect. C: Struct. Chem.* **2015**, *71*, 3-8.

49. Farrugia, L. J. *WinGX* and *ORTEP for Windows*: an update. *J. Appl. Crystallogr*. **2012**, *45*, 849-854.

50. Macrae, C. F.; Edgington, P. R.; McCabe, P.; Pidcock, E.; Shields, G. P.; Taylor, R.; Towler, M.; van de Streek, J. *Mercury:* visualization and analysis of crystal structures. *J. Appl. Crystallogr*. **2006**, *39*, 453-457.

51. Dolomanov, O. V.; Bourhis, L. J.; Gildea, R. J.; Howard, J. A. K.; Puschmann, H. *OLEX2*: a complete structure solution, refinement and analysis program. *J. Appl. Crystallogr*. **2009**, *42*, 339-341.

For Table of Contents Use Only

Conformational Solvatomorphism in a [2]Catenane

Shobhana Krishnaswamy,[a] Soumyakanta Prusty,[a] Daniel Chartrand,[b] Garry S. Hanan[b] and Dillip K. Chand*[a]

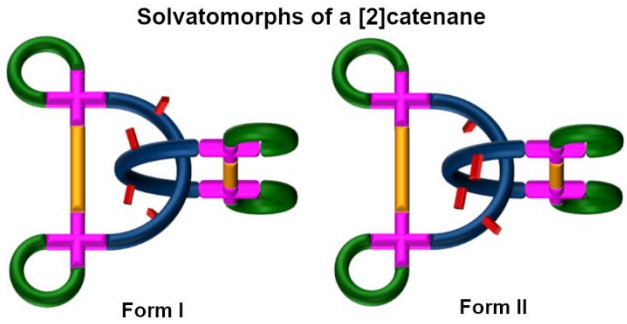

A [2]catenane formed using a combination of a flexible pyridine-appended ligand, a rigid pyridine-appended ligand and Pd(phen)$(NO_3)_2$, yielded conformational solvatomorphs upon crystallization from acetonitrile-water. These solvatomorphs showed subtle differences in the orientation of the amide carbonyl groups of the ligand units in the macrocycles with associated changes in the hydrogen bonding interactions between the catenating rings.